Using CDE 2-layer Test Data to Evaluate Geometric Product of Diode Signals as Single CDE Energy Estimator

Mark Strickman
24Aug2004

1. Introduction

In the past, calibration reconstruction has used the arithmetic mean of the signal from the two ends of a hit CDE to estimate the energy deposited in that CDE ((Plus + Minus)/2). This estimator is independent of where along the crystal the energy deposition occurred, given the approximations that the light yield as a function of position (also known as light taper or light attenuation) is linear, and that the slopes of the light yield curves from either end are equal.

More recently, we have considered changing the single CDE energy estimator to the geometric mean of CDE end signals (SQRT(Plus*Minus)). This is the correct approach if, instead of a linear light yield curve, the crystals have an exponential curve. In this case, the geometric mean is independent of position if the efolding lengths are the same for both ends.

In reality, none of these assumptions are rigorously true for all CDEs. The light attenuation curve is typically some combination of linear and exponential components and, furthermore, changes from CDE to CDE.

We now have enough test data to conclusively test the results of these assumptions. In particular, we can look at the deviations of the energy estimators from a constant for energy deposition at various positions along the crystal. In addition, we can study the differences between big and small (i.e. low energy and high energy) PIN diodes in these respects.

2. Test Setup and Data

These tests use flight CDE test data measured as part of the post CDE manufacture testing process at Swales Aerospace. The test configuration is a two-layer hodoscope, the top layer of which contains the twelve test CDEs and the bottom the twelve fiducial CDEs. By requiring no more than a single CDE muon hit in each layer, the range of incident angles for the muon, and, hence, the range of path lengths, is restricted by the geometry of the layers.The CDEs at the edge of each layer have a somewhat broader distribution of path lengths since they have no way to reject events exiting the side of the crystal on the side with no adjacent CDE.

This arrangement defines 12 longitudinal “slices” for each test CDE, corresponding to events with a hit in the test CDE plus a hit in one of the 12 fiducial CDEs below. Each slice is roughly 27 mm long, corresponding to the width of the fiducial CDE.

The tests are run by an on-line GSE process. Analysis consists of collecting single slice spectra from both PINs (the small PIN is set up in muon gain mode so as to have a usable signal) from the plus and minus ends of each CDE. The spectra are then fit using a log-normal model (which accounts, to some extent, for the non-landau shape of the peak brought about by the path length distribution and other effects). A variety of quantities, such as light yield and asymmetry are computed from the resulting most probable values and stored in csv files in \\glastserv\glast2\FM\CdeData\Database*.csv. Each csv file contains the results of a single run, consisting of parameters for each of 12 test CDEs.

3. <u>Analysis</u>

Analysis of the CDE test data is performed in two steps, single CDE analysis and statistical analysis.

3.1. Single CDE Analysis

The first step used **plotCdeSlices_big_vs_small c.pro** (in IDL v.6) to read in each CDE and analyze the results into a set of plots per CDE. The *deviations* keyword turns the lower two plots on and off, while the *stat* keyword can be set to GEOMETRIC or ARITHMETIC depending on whether geometric mean or arithmetic mean energy calculation is desired. The *prodstats* keyword can be assigned a variable that will contain an array of statistics for each CDE, including standard deviation and maximum deviations for the fluctuations of energy from a constant as a function of position along the crystal.

The analysis code for these results generates the following plots and statistics for each CDE (one run of the code will use either geometric or arithmetic means):

Upper Left Plot:

1. Light yield, normalized to the mean light yield, vs slice, for each PIN (big and small) from each CDE end
2. Linear fit to each of the above
3. Arithmetic or geometric mean of the two ends for big PIN, small PIN, and one of each ("mixed" PINs)

Lower Left Plot:

1. Residuals of the big PIN light yields from the linear fit model vs slice
2. Residuals of the arithmetic or geometric mean of the ends from a constant set to their mean value over all slices (which is 1 by construction) vs slice
3. Standard deviation, maximum deviation, and maximum deviation excluding the end slices of the mean residuals discussed in 2 above.

Lower Right Plot

1. Same as 1,2,3 in the Lower Left Plot, for the small PIN
2. Same as 2,3 in the Lower Left Plot, for "mixed" PINs

Upper Right Plot

1. Asymmetry curve (log (P/M) vs slice) for big PIN, small PIN and "mixed" PINs

3.2. Statistical Analysis

The second analysis step uses the program **histostats.pro**, which reads in the aforementioned array of statistics from the previous analysis (produced using the *prodstats* keyword), histograms the stats and plots the histograms. For each of big PINs, small PINs and "mixed" PINs, histograms of standard deviation from a constant vs position, maximum deviation, and maximum deviation excluding the end slices are all plotted.

4. Results

Figures 1 and 2 show sample plots for the same CDE for the geometric (Figure 1) and arithmetic (Figure 2) mean energy estimators.

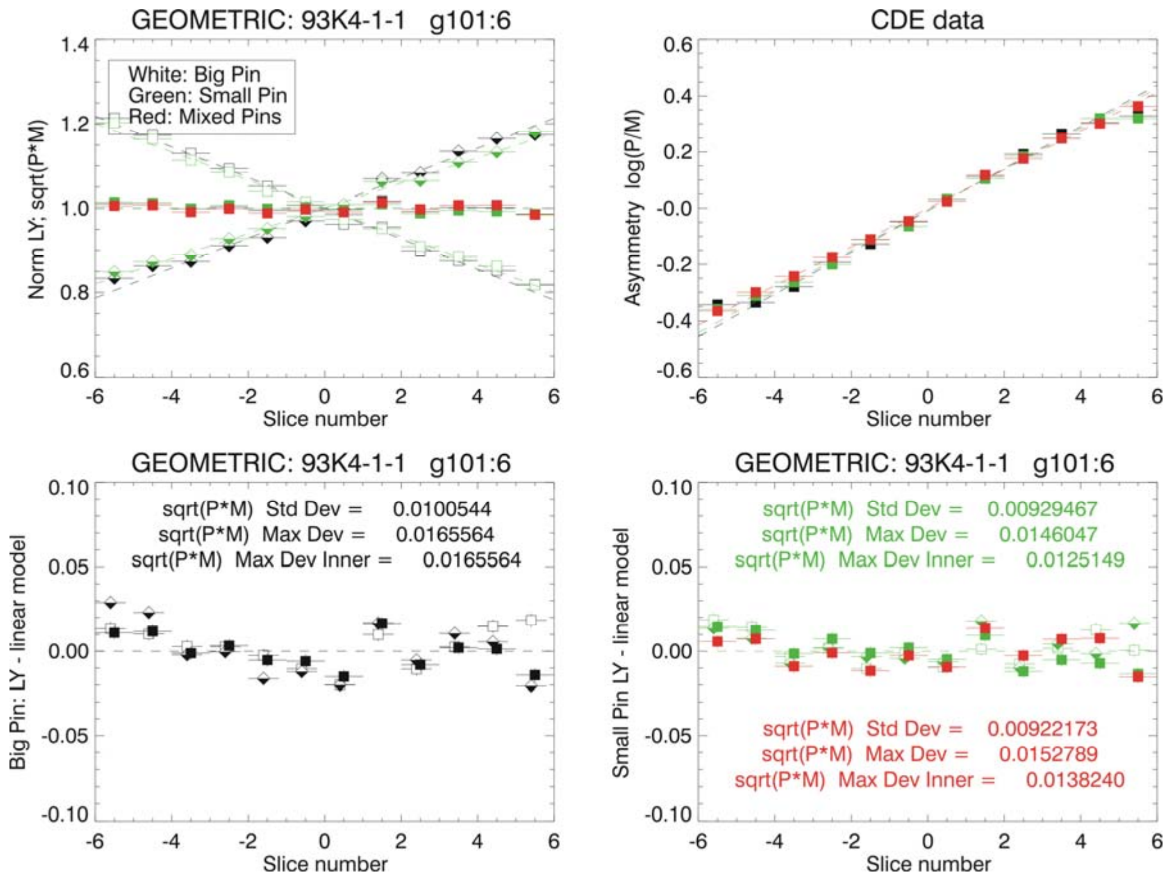

Figure 1 Single CDE light yield and energy estimation using geometric mean of ends

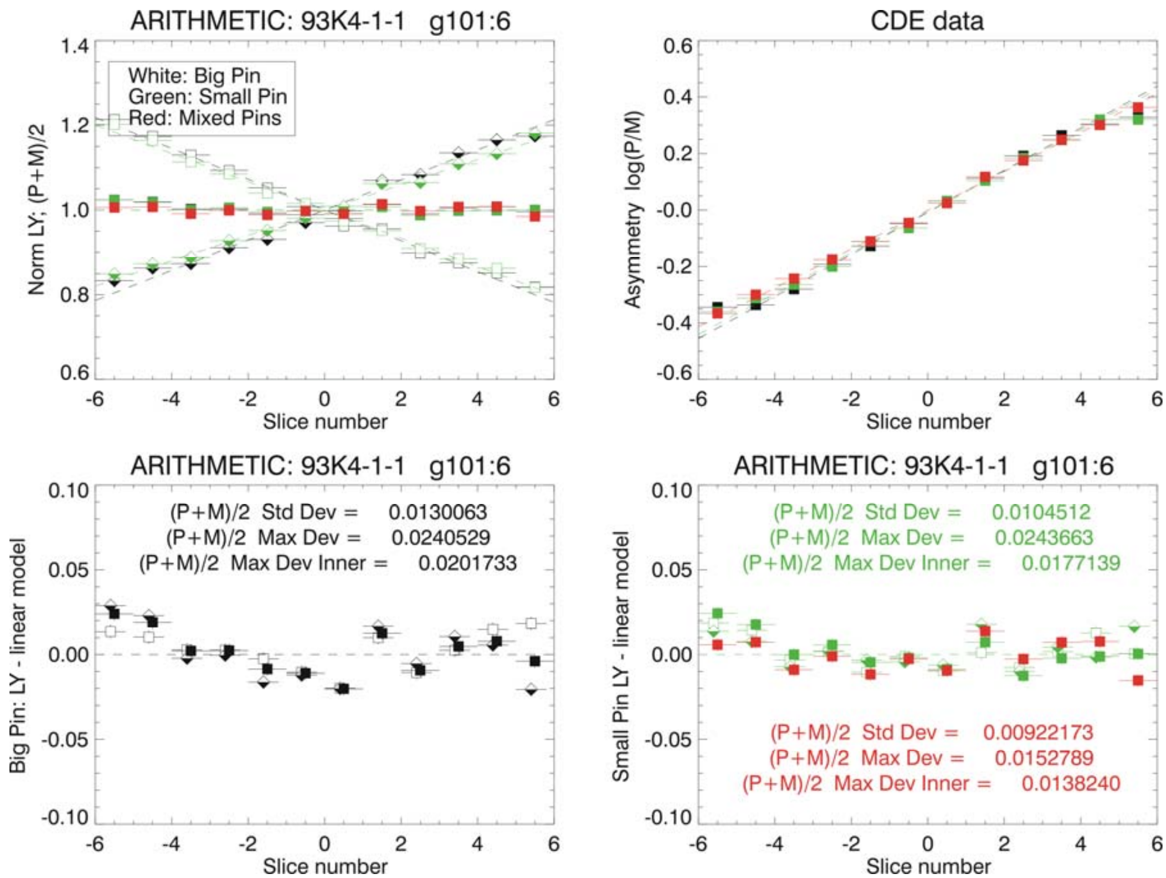

Figure 2 Single CDE light yield and energy estimation using arithmetic mean of ends

The big and small PIN light yield curves are not necessarily the same. Typically, the small PIN light yield shows less slope as a function of position than that of the big PIN. This may be due to differences in direct vs diffuse illumination of the two PINs. In Figure 2, note that the small PIN light yield has less slope than the big PIN except in the lower right quadrant (high slice number, far from PIN), where the two are virtually identical. This asymmetric behavior is not unusual.

Despite this behavior, though, the assumption that the geometric mean as an energy estimator is independent of energy deposit position is a remarkably good one. Even in the case of “mixed” PINs i.e. when we use the large PIN from one end and the small from the other end, the fluctuations of the geometric mean are less than 2%. The performance of the arithmetic mean is also acceptable, although not quite as good.

Also, as we have assumed in the past, the asymmetry curves are rather linear except near the ends of the crystal. Our new muon calibration scheme no longer depends on linearity of the asymmetry curves. Instead, it stores a cubic spline representation of the curve, which can reproduce any functional behavior.

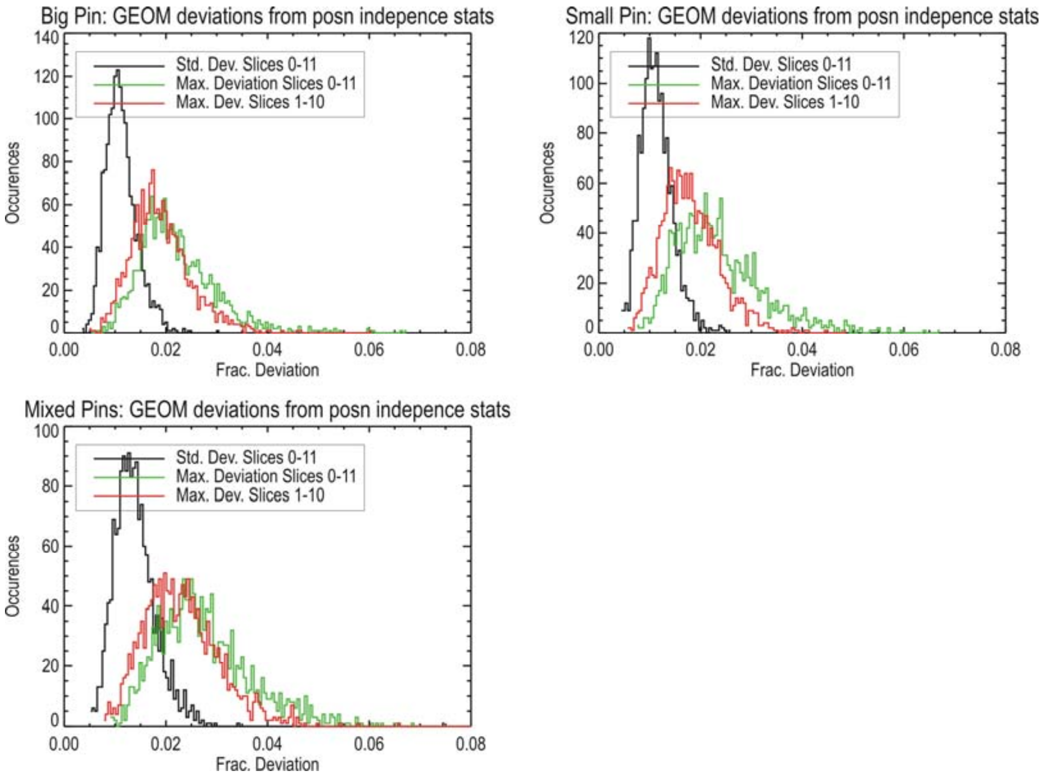

Figure 3 Statistics on deviations of geometric mean energy estimator from position independence.

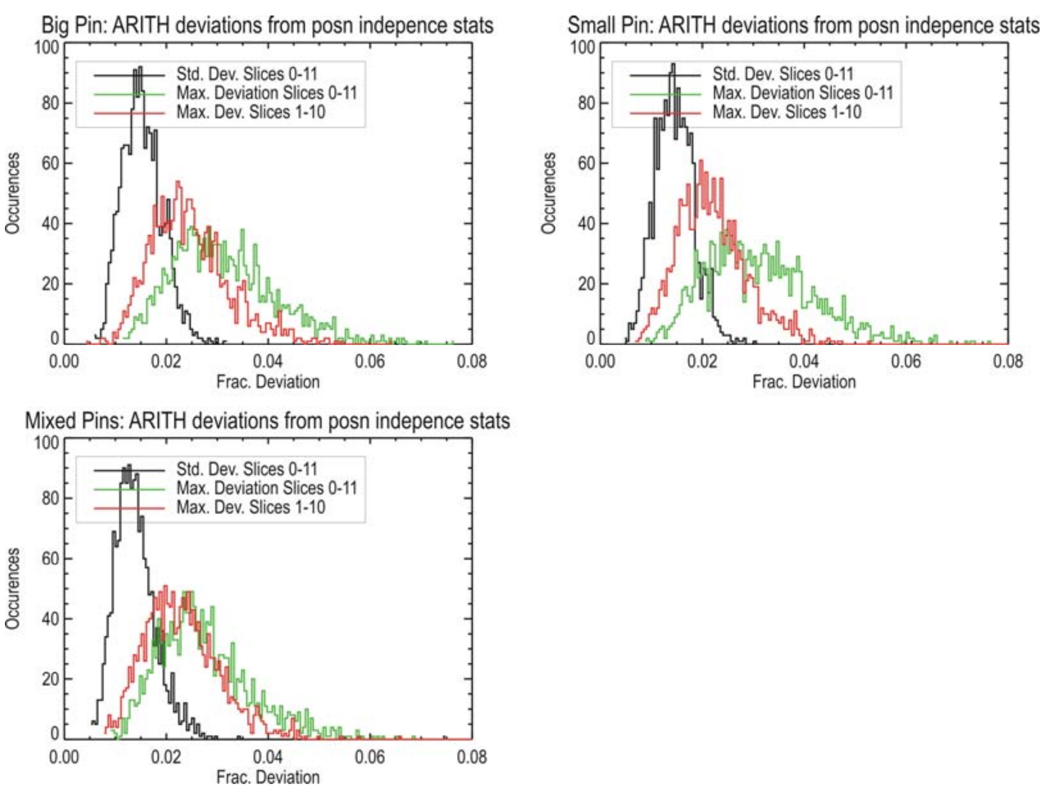

Figure 4 Statistics on deviations of arithmetic mean energy estimator from position independence.

Figure 3 and Figure 4 show statistics of how well the assumption that each energy estimator is independent of position holds up over 1620 flight CDEs. In all cases, the most probably standard deviation is well below 2%. The geometric mean estimator fluctuates from a constant vs position with a standard deviation ~1%, while the arithmetic mean estimator is at ~1.5%. These numbers do not change very significantly for different PIN configurations (big PIN, small PIN or mixed PINs).

The maximum deviations are a little worse for the arithmetic mean estimator, extending out to about 6% for the big PIN, as opposed to about 4% for the big PIN using the geometric mean estimator.

5. Conclusion

We believe that these tests indicate that the assumption that either the geometric mean energy estimator or the arithmetic mean estimator is independent of energy deposition position is valid to within required precision. The geometric mean estimator is somewhat the better of the two, especially when considering maximum deviations from the assumption of position independence.

While deviations from constant are noticeably worse near the ends of the crystal, at the position resolution of these data, they are still small enough to be acceptable. Further study of the behavior of these estimators near the crystal ends, using better position resolution based on TKR information, is in progress.